Journal of Molecular Structure 1120 (2016) 281–293

Contents lists available at ScienceDirect

Journal of Molecular Structure

journal homepage: http://www.elsevier.com/locate/molstruc

Polymorphism in chloro derivatives of 1,4-naphthoquinone: Experiment and density functional theoretic investigations

Dinkar Chaudhari [a], Shridhar P. Gejji [a, **], Dipali N. Lande [a], Debamitra Chakravarty [b], Sunita Salunke-Gawali [a, *]

[a] Department of Chemistry, Savitribai Phule Pune University, Pune 411007, India
[b] Central Instrumentation Facility, Department of Chemistry, Savitribai Phule Pune University, Pune 411007, India

ARTICLE INFO

Article history:
Received 22 March 2016
Received in revised form
6 May 2016
Accepted 9 May 2016
Available online 12 May 2016

Keywords:
Polymorphism
Naphthoquinone
π-π stacking
Hydrogen bonding
Dichlone
TD-DFT

ABSTRACT

Molecular interactions underlying polymorphs of chlorine containing 1,4-naphthoquinone derivatives have been investigated by employing single crystal X-ray, ^{1}H NMR, FTIR and electronic spectra experiments combined with density functional theory. Two polymorphs of 2,3-dichloro-1,4-naphthoquinone possessing (i) triclinic space group *P-1*(**A1** and **A3**), and (ii) orthorhombic with $Pb2_1a$ (**A2**) space group were obtained. The polymorph A3 has two molecules in its asymmetric unit which facilitate C–H···O interactions engendeing polymeric planar sheets. The two polymorphs of 2-amino-3-chloro-1,4-naphthoquinone reveal monoclinic forms with *Pc* (B1) and $C_{2/c}$ (B2) space groups. A tetramer of B2 molecule possess N–H···O interactions. The polymorphs of 2-chloro-3-hydroxy-1,4-naphthoquinone crystallizes in monoclinic space groups *Pc* (C1) and *Pn* (C2). Polymeric chain of C2 molecules results via O–H···O interactions and the chains further are connected through C–H···Cl and π-π stacking interactions those arise from benzenoid and quinonoid centroid. Moreover A3 facilitates the dimer via the halogen bonding interactions. Furthermore hydrogen bonding renders stability to the dimer C2. On the other hand compound B2 does not favor dimer formation. These inferences based on experimental observations are rationalized through the use of the dispersion corrected M06-2x functional based density functional theory. Further time dependent density functional theory has been used to assign the electronic transitions in UV–visible spectra of A3, B2 and C2.

1. Introduction

Polymorphism in crystalline solids or materials has same chemical composition with different lattice structures and/or different molecular conformations. Molecular arrangement in crystalline solids are facilitated through noncovalent interactions such as hydrogen bonding, van der Waals interactions, π-π stacking and electrostatic interactions [1]. Hydrogen bonding has been one of the key factors toward noncovalent binding that has been explored for molecular recognition [2,3]. Such non covalent interactions control the chemical stability, solubility and the bioavailability of the active pharmaceutical ingredients [4] in pharmaceutical solids.

The biological applications of quinone molecules include as antibiotics [5], anticancer [6,7], vitamin [8], antibacterial [9], fungicide [10] etc. Innumerable quinone compounds studied by crystallography revealed hydrogen bonding interactions. The weak molecular interactions engender polymorphic structures in quinones [11–16]. Molecular interactions responsible for drug action in particular, those between drug or biomolecules have been of fundamental importance. With this motif the polymorphs of chloro derivatives of 1,4-naphthoquinones viz., 2,3-dichloro-1,4-naphthoquinone(polymorphs A1 to A3), 2-amino-3-chloro-1,4-naphthoquinone (polymorphs B1 and B2) and 2-chloro-3-hydroxy-1,4-naphthoquinone (polymorphs C1 and C2) (Table 1) have been investigated in the present work. Interestingly 2,3-dichloro-1,4-naphthoquinone commonly known as dichlone was first synthesized by Graebe [19] in 1867 and described by Carstanjen [20] in following year finds applications as algicide [17] and fungicide [18]. Besides dichlone serves as DNA methyl transferase inhibitor [21] and can be exported as starting material for synthesis

* Corresponding author.
** Corresponding author.
E-mail addresses: spgejji@chem.unipune.ac.in (S.P. Gejji), sunitas@chem.unipune.ac.in (S. Salunke-Gawali).

http://dx.doi.org/10.1016/j.molstruc.2016.05.022
0022-2860/

Table 1
Details of polymorphs A1 to A3, B1, B2 and C1, C2.

Compound	Molecular structure	Polymorph	Space group	Reference
2,3-dichloro-1,4-naphthoquinone (Dichlone)	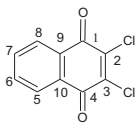	A1	Triclinic *P-1*	[26]
		A2	Orthorhombic *Pb2$_1$a*	[27]
		A3	Triclinic *P-1*	Present work
2-amino-3-chloro-1,4-naphthoquinone	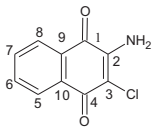	B1	Monoclinic *Pc*	[31]
		B2	Monoclinic *C2/c*	Present work
2-chloro-3-hydroxy-1,4-naphthoquinone (Chlorolawsone)	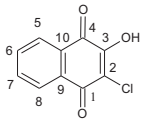	C1	Monoclinic *Pn*	[29]
		C2	Monoclinic *C2/c*	Present work

of numerous compounds of biological significance [22]. Dichlone further has been utilized in nucleophilic substitution reactions [23,24] and also in synthesis of numerous heterocyclic compounds [25]. The crystal structure of dichlone was elucidated in 1961 [26], the crystals grown in toluene revealed triclinic space group (A1) (Table 1). On the other hand, the crystals grown from the compound melt showed orthorhombic space group (A2) [27]. The works of Hauw et al. [29] further concluded that in alkaline and neutral solutions dichlone hydrolyzes to form 2-chloro-3-hydroxy-1,4-naphthoquinone [28]; the single crystal X-ray data of which was elucidated only in 1965 (C1). Fries et al. [30] carried out the synthesis of 2-amino-3-chloro-1,4-naphthoquinone the structure of which was known since 1965 (B1) [31].

All three compounds studied in present investigation were used to synthesize several compounds those find application in pharmacology and in medicinal chemistry. Despite of all these experimental studies the reports on the molecular interactions in different polymorphs of these compounds are rather limited. The present work precisely focuses on this aspect and outlines analysis of structural and spectral characteristics of biologically as well as synthetically important chlorine containing 1,4-naphthoquinone derivatives (Table 1).

2. Experimental section

2.1. General materials and methods

The materials used viz., 2,3-dichloro-1,4-naphthoquinone was purchased from Sigma-Aldrich and used as received. KOH pellets and aqueous ammonia was obtained from Merck chemicals. Analytical grade solvents used such as dichloromethane, toluene, methanol, pet ether, ethyl acetate were purchased from Merck Chemicals. Solvents were distilled by standard methods [32] and dried wherever necessary. FT-IR spectra were recorded between 4000 and 400 cm^{-1} as KBr pellets on SHIMADZU FT 8400 Spectrophotometer. Melting points of compounds were determined using (Make-METTLER). ^1H (500 MHz) and ^{13}C (125 MHz) NMR of compound B2 was recorded in DMSO-d_6, on Varian 500 MHz NMR instrument. TMS (tetramethylsilane) was used as the reference. UV–visible spectra of all compounds in methanol were recorded from 200 nm to 800 nm on Shimadzu UV 1800 spectrophotometer.

2.2. Synthesis of 2-amino-3-chloro-1,4-naphthoquinone; B2

Modified procedure have been used for synthesis of 2-amino-3-chloro-1,4-naphthoquinone [33]. Recrystallized 2,3-dichloro-1,4-naphthoquinone, (0.5 g, 2.2 mM) was suspended in 20 ml of ethanol and 25 ml ammonium hydroxide solution was added to the solution of dichlone with constant magnetic stirring. The mixture was refluxed for 3 h at 60 °C. Red color precipitate was obtained, which was filtered and washed with diethyl ether and dried in vacuum. The product was further purified by column chromatography (silica column, 60–120 mesh) and eluted with pet ether/ethyl acetate.

2.3. Synthesis of 2-chloro-3-hydroxy 1,4-naphthoqinone; C2

Modified procedure [28] has been used for synthesis of compound 'C2'. Recrystallized 2,3-dichloro-1,4-naphthoquinone (0.5 g, 2.2 mM) have been added in 10 ml of water. To this suspension, 10 ml aqueous solution of KOH (0.247 g, 4.4 mM) was added with constant magnetic stirring. This reaction mixture was heated for ~1 h at 70 °C. Red color solution was obtained. Unreacted dichlone was extracted with dichloromethane from aqueous reaction mixture and was acidified by adding a few drops of concentrated hydrochloric acid till pH of the reaction mixture becomes acidic (pH = 2). Yellow color precipitate thus obtained was filtered and washed with diethyl ether and dried in vacuum. This yellow color residue was further purified by column chromatography (silica column, 60–120 mesh) and eluted with ethyl acetate/pet ether (1:9). X-ray quality crystals were obtained after recrystallization of solid product in methanol.

2.4. Characterization

2-amino-3-chloro-1,4-naphthoquinone; B2. Red crystal, Yield: 0.342 g (79.93%). m. p 195–196 °C. FT-IR (KBr, $\nu_{max}(cm^{-1})$): 3403, 3293, 2322, 2287, 1678, 1590, 1553, 1305, 1268, 711, 685, 592, 521.^1H NMR (500 MHz, DMSO-d_6, δ (ppm)): 8.17 (d, 1H, J = 7.5 Hz), 8.16 (d, 1H, J = 7.5), 7.7 (t, 1H, J = 7.5), 7.65 (t, 1H, J = 7.65), 5.5 (s, 2H). ^{13}C NMR (125 MHz, DMSO-d_6, δ(ppm)): 176, 145, 134, 132, 132, 129, 126, 126. UV–vis (λ_{max} (nm), methanol): 284, 332, 449.

2-hydroxy-3-chloro-1,4-naphthoqinone; C2. Yellow Solid, Yield: 0.400 g (87.14%). m. p. 206–207 °C. FT-IR (KBr, $\nu_{max}(cm^{-1})$): 3269, 1668, 1639, 1585, 1454, 1363, 1330, 1298, 1273, 1219, 1128, 1008,

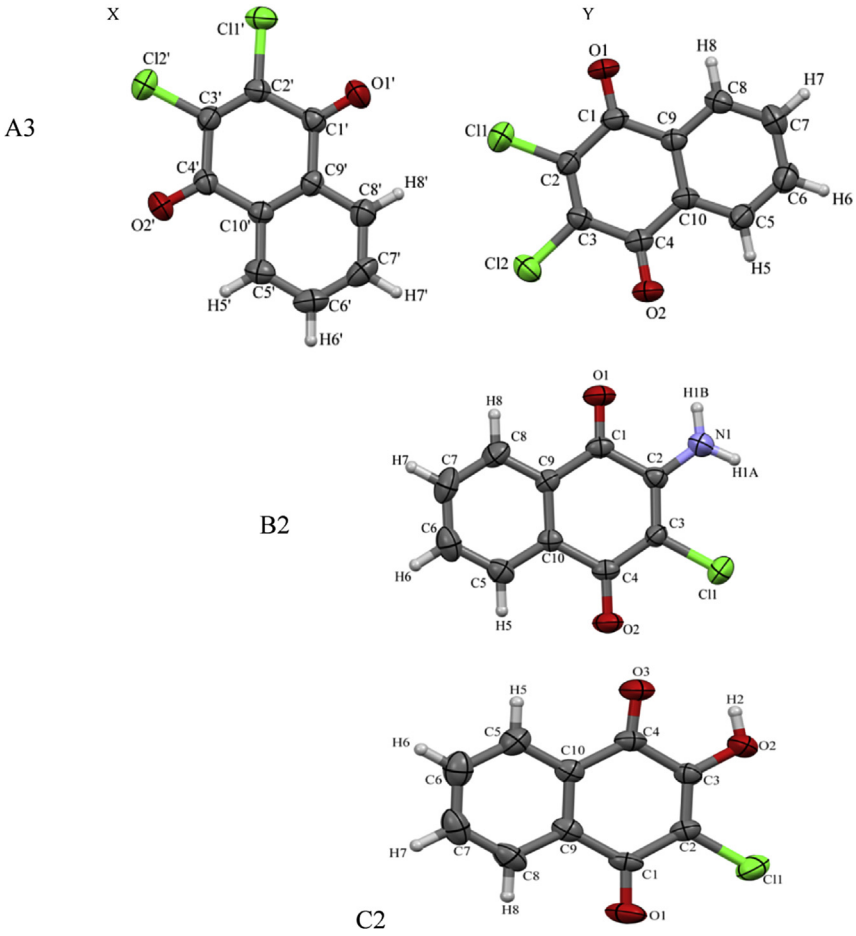

Fig. 1. ORTEP plot of compound A3, B2 and C2. The ellipsoid was drawn with 50% probability.

Table 2
Crystallography parameters of A3, B2 and C2.

	A3	B2	C2
CCDC	1426674	1426672	1426673
Empirical formula	$C_{20}H_8\ Cl_4\ O_4$	$C_{10}\ H_6Cl\ NO_2$	$C_{10}\ H_5Cl\ O_3$
Formula weight	454.06	207.61	208.59
Temperature	296(2) K	296(2) K	296(2) K
Wavelength	0.71073 Å	0.71073 Å	0.71073 Å
Crystal system, space group	Triclinic, *P-1*	Monoclinic, *C2/c*	Monoclinic, *P n*
Unit cell dimensions	a = 7.32790(10) Å,	a = 13.7381(3) Å,	a = 8.25530(15) Å,
	α = 89.7690(6)°	α = 90.0°	α = 90.0°
	b = 8.27650(10) Å,	b = 7.57140(10)Å,	b = 3.90730(7)Å,
	β = 82.5420(10)°	β = 110.7030(7)°	β = 100.4200(8)°
	c = 16.1368(3) Å,	c = 18.2389(3) Å,	c = 13.4222(2) Å,
	γ = 67.0180(10)°	γ = 90.0°	γ = 90.0°
Volume	892.22(2) $Å^3$	1774.64(5)$Å^3$	425.806(13)$Å^3$
Z, Calculated density	2, 1.690 Mg/m^3	8, 1.554 Mg/m^3	2, 1.627 Mg/m^3
Absorption coefficient	0.690 mm^{-1}	0.397 mm^{-1}	0.420 mm^{-1}
F(000)	456	848	212
Crystal size	0.49 × 0.48 × 0.27 mm	0.492 × 0.473 × 0.264 mm	0.49 × 0.47 × 0.26 mm
Theta range for data collection	2.905–28.400°	3.123–28.405°	3.086–28.328°
Limiting indices	−9 ≤ h<=9, −11 ≤ k<=10, −21 ≤ l<=21	−18 ≤ h<=18, −10 ≤ k<=10, −24 ≤ l<=24	−10 ≤ h<=11, −5 ≤ k<=5, −17 ≤ l<=17
Reflections collected/unique	30738/4409 [R(int) = 0.0500]	32282/2225 [R(int) = 0.0975]	10250/2114 [R(int) = 0.0534]
Completeness to theta = 30.49	99.9%	99.9%	99.9%
Absorption correction	Semi-empirical from equivalents	MULTI SCAN	Semi-empirical from equivalents
Max. and min. transmission	0.830 and 0.720	0.9024 and 0.8285	–
Refinement method	Full-matrix least-squares on F^2	Full-matrix least-squares on F^2	Full-matrix least-squares on F^2
Data/restraints/parameters	4409/0/254	1558/0/128	2225/0/127
Goodness-of-fit on F^2	1.023	0.998	1.05
Final R indices [I > 2sigma(I)]	R1 = 0.0474, wR2 = 0.0922	R1 = 0.0497, wR2 = 0.0980	R1 = 0.0351, wR2 = 0.0570
R indices (all data)	R1 = 0.0911, wR2 = 0.1107	R1 = 0.0970, wR2 = 0.1172	R1 = 0.0510, wR2 = 0.0602
Largest diff. peak and hole	0.268 and −0.346 $e.A^{-3}$	0.271 and −0.209 e. A^{-3}	0.185 and −0.153 e. A^{-3}

Table 3
Hydrogen bonding interactions of A2, A3, B2 and C2.

Compound	D-H···A	D···H(Å)	H···A(Å)	D···A(Å)	D- H···A(°)
A3	C(8)–H(8)···Cl(2)$^{(i)}$	0.929	2.827	3.736(3)	166.0
	C(7′)–H(7′)···O(1)$^{(ii)}$	0.930	2.612	3.450(4)	150.1
	C(6′)–H(6′)···Cl(1)$^{(ii)}$	0.931	2.847	3.727(3)	157.9
	C(7)–H(7)···Cl(2)$^{(iii)}$	0.930	2.868	3.704(3)	165.1
	C(5)–H(5)···Cl(2′)$^{(iv)}$	0.930	2.882	3.805(3)	172.6
	C(6)–H(6)···O(2′)$^{(iii)}$	0.930	2.643	3.490(4)	151.6
	C(7)–H(7)···Cl(2′)$^{(iii)}$	0.930	2.868	3.704(4)	150.2
	C(5′)–H(5′)···Cl(1)$^{(i)}$	0.930	2.887	3.808(4)	170.7
	C(8′)–H(8′)···Cl(1)$^{(v)}$	0.930	2.883	3.789(4)	165.1
B2	N(1)–H(1B)···O(2)$^{(vi}$	0.860	2.408	3.167(2)	147.5
	N(1)–H(1A)···O(2)$^{(vii)}$	0.860	2.323	3.153(2)	162.5
	C(8)–H(8)···Cl(1)$^{(viii)}$	0.930	2.810	3.643(2)	149.6
	C(5)–H(5)···O(1)$^{(vi)}$	0.931	2.331	3.187(3)	152.7
C2	C(5)–H(5)···Cl(1)$^{(ix)}$	0.930	2.890	3.563(3)	130.1
	C(8)–H(8)···O(3)$^{(x)}$	0.931	2.546	3.295(3)	137.8
	O(2)–H(2)···O(1)$^{(xi)}$	0.820	2.046	2.770(2)	147.0
A2	C(6)–H(4)···O(1)$^{(xii)}$	0.917	2.639	3.391	139.7
	C(16)–H(2)···O(2)$^{(xiii)}$	1.040	2.701	3.592	143.4
	C(17)–H(7)···O(4)$^{(xiv)}$	0.909	2.606	3.337	137.8
	C(16)–H(2)···Cl(1)$^{(v)}$	1.040	2.937	3.751	135.4
	C(3)–Cl(2)···O(4)$^{(xv)}$	1.726	3.252		151.6
	C(12)–Cl(3)···O(1)$^{(xvi)}$	1.694	3.169		166.3
	C(2)–Cl(1)···O(2)$^{(xvii)}$	1.701	3.159		167.9

(i) x,−1+y,z; (ii) x,1+y,z (iii) x,1+y,1+z; i½v) x,y,1+z ; v) x,y,z, vi) −½+x,−½+y,z; vii) ½−x,− ½+y, ½−z; viii) x,2−y,−½+z; ix) −1+x,1+y,z ; x) −½+x,−y,−½+z; xi) −½+x,1−y,−½+z; (xii) −½+x,y,z; (xiii) ½+x,y,−1−z; xiv) ½+x,y,z; xv) x,y,−1+z; xvi) ½−x,−½+y,−1+z; xvii) ½+x,y−1,−1−z.

856, 727, 682, 599, 538. ^{1}H NMR (400 MHz, DMSO-d_6, δ (ppm)): 8.00 (dd, 2H), 7.86–7.74 (m, 2H), 3.89 (s, 1H). ^{13}C NMR (100 MHz, DMSO-d_6, δ (ppm)): 180.74, 178.26, 158.53, 135.22, 133.79, 132.30, 130.10, 126.77, 126.59, 126.11. UV–vis (λ_{max} (nm), methanol): 287, 321, 473.

2.5. X-ray crystallography

The X-ray quality yellow-green crystals of compound 'A3' was obtained from the unreacted fraction from the column of the reaction between 2,3-dichloro-1,4-naphthoquinone and 2-aminophenol. A red block crystal of 'B2' was obtained after evaporation of red fraction of the column and a yellow block crystal of 'C2' was obtained after evaporation of methanol solution. Crystals of appropriate size were chosen for data collection.

Data for all three compounds have been collected on D8 Venture PHOTON 100 CMOS diffractometer using graphite monochromatized Mo-K_α radiation (λ = 0.7107 Å) with exposure/frame = 8 s, 15 s and 10 s for A3, B2 and C2 respectively. The X-ray generator was operated at 50 kV and 30 mA. An initial set of cell constants and an orientation matrix were calculated from total 24 frames. The optimized strategy used for data collection consisted different sets of ϕ and ω scans with 0.5° steps in ϕ/ω. Crystal to detector distance was 5.00 cm with 512 × 512 pixels/frame, Oscillation/frame −0.5°, maximum detector swing angle = −30.0°, beam centre = (260.2, 252.5), in plane spot width = 1.24. Data integration was carried out by Bruker SAINT program and empirical absorption correction for intensity data were carried out by Bruker SADABS. The programs are integrated in APEX II package [34]. The data were corrected for Lorentz and polarization effect. The structure was solved by *Direct Method* using SHELX-97 [35]. The final refinement of the structure was performed by full-matrix least-squares techniques with anisotropic thermal data for non-hydrogen atoms on F^2. The non-hydrogen atoms were refined anisotropically whereas the hydrogen atoms were refined at calculated positions as riding atoms with isotropic displacement parameters. Molecular diagrams were generated using ORTEP-3 [36] and Mercury programs [37]. Geometrical calculations were performed using SHELXTL [35] and PLATON [38].

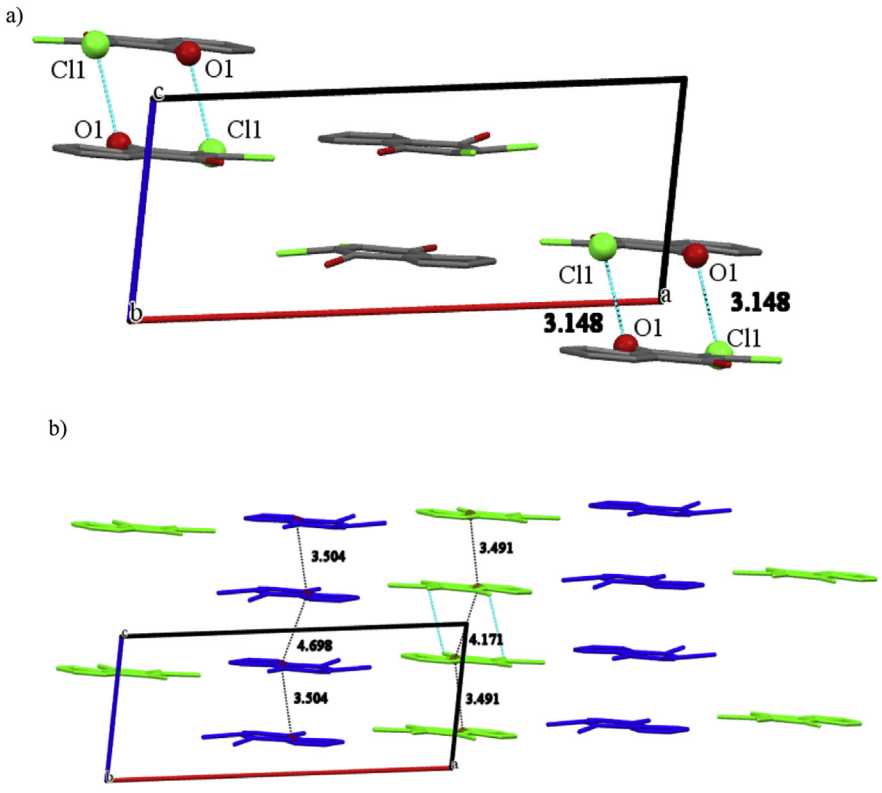

Fig. 2. Dichlone molecules of triclinic space group *P-1* (A1) showing a) π-π stacking and b) Cl···O close contacts down b-axis.

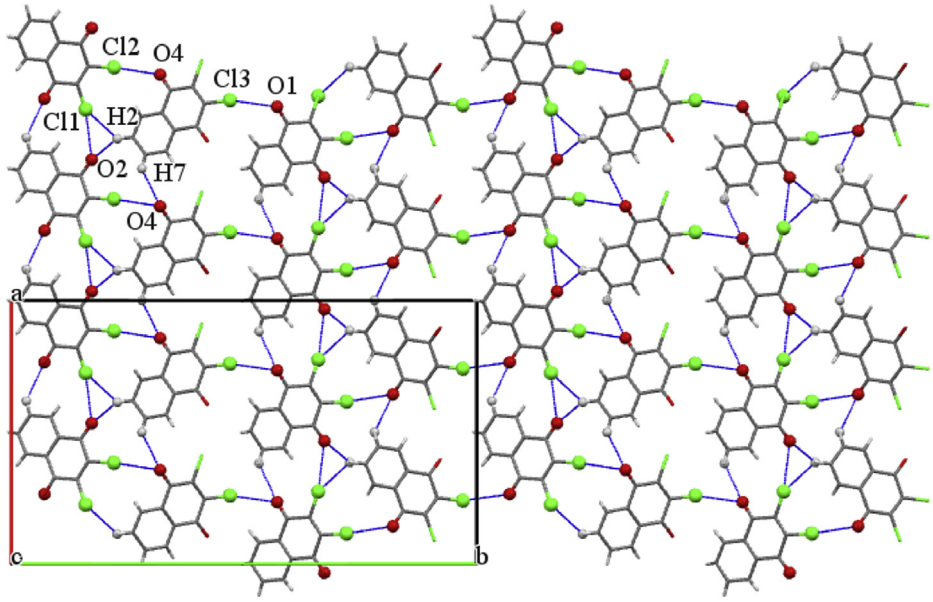

Fig. 3. Dichlone molecules of orthorhombic space group ($Pb2_1a$)(A2) showing polymer of dimeric units of 'X1' and 'Y1' down c-axis.

2.6. Computational details

Optimized structures of A3, B2 and C2 were derived within the framework of M06-2x based density functional theory employing the Gaussian-09 program [39]. The internally stored 6-31G basis set with diffuse functions being added on all the heavy atoms (designated as 6-31++G(d,p) basis) have been used for optimizations [40–42]. The stationary point structures were confirmed to be local minima on the potential energy surface through vibrational frequency calculations. Frontier orbital were computed in the same framework of theory.

3. Result and discussion

3.1. Molecular interactions in polymorphs A1–A3, B1–B2 and C1–C2

The ORTEP plots of polymorphs A3, B2 and C2 are shown in Fig. 1. The crystallographic data is presented in Table 2. Hydrogen bonding parameters are reported in Table 3. The molecular interactions of A3, B2 and C2 together with respective known polymorphs in literature are outlined below.

3.2. Polymorphs A1 to A3

Two polymorphic structures of dichlone were known prior to this report. These polymorphs are designated by A1 [26] and A2

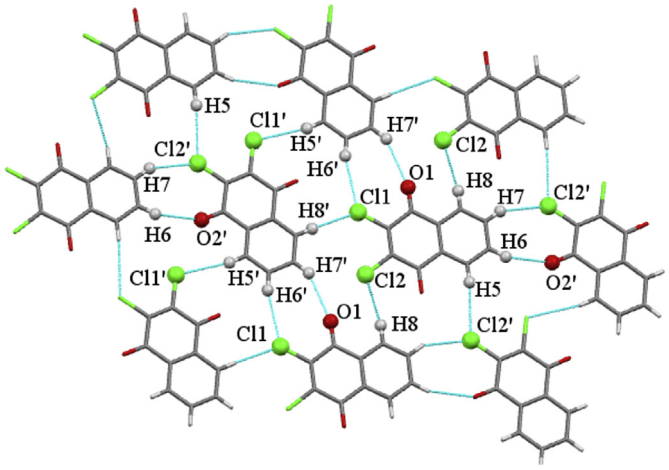

Fig. 4. Planar polymeric sheets of Dichlone in triclinic *P-1* space group (A3) formed by C–H···O and C–H···Cl interactions of 'X' and 'Y' molecules.

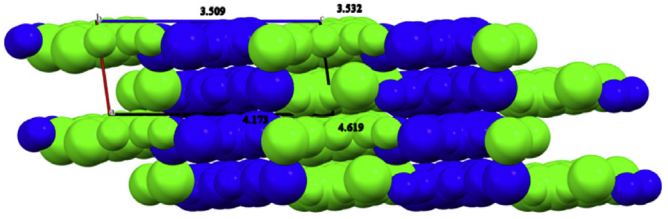

Fig. 5. π···π stacking of symmetry equivalent molecule X (green, 3.532 Å) and Y (Blue, 3.509 Å) molecules down b-axis. The interlayer spacing between π&ctdotπ stacked molecules; green (centroid separation being 4.619 Å), blue (centroid distance being 4.173 Å).

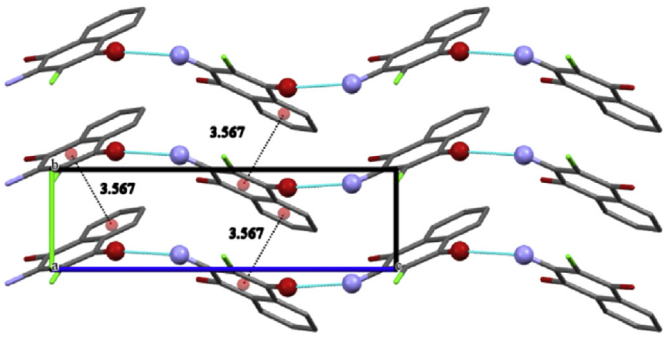

Fig. 6. Polymeric chain π-π stacked chains of compound 'B1' formed by N–H···O interaction down a-axis.

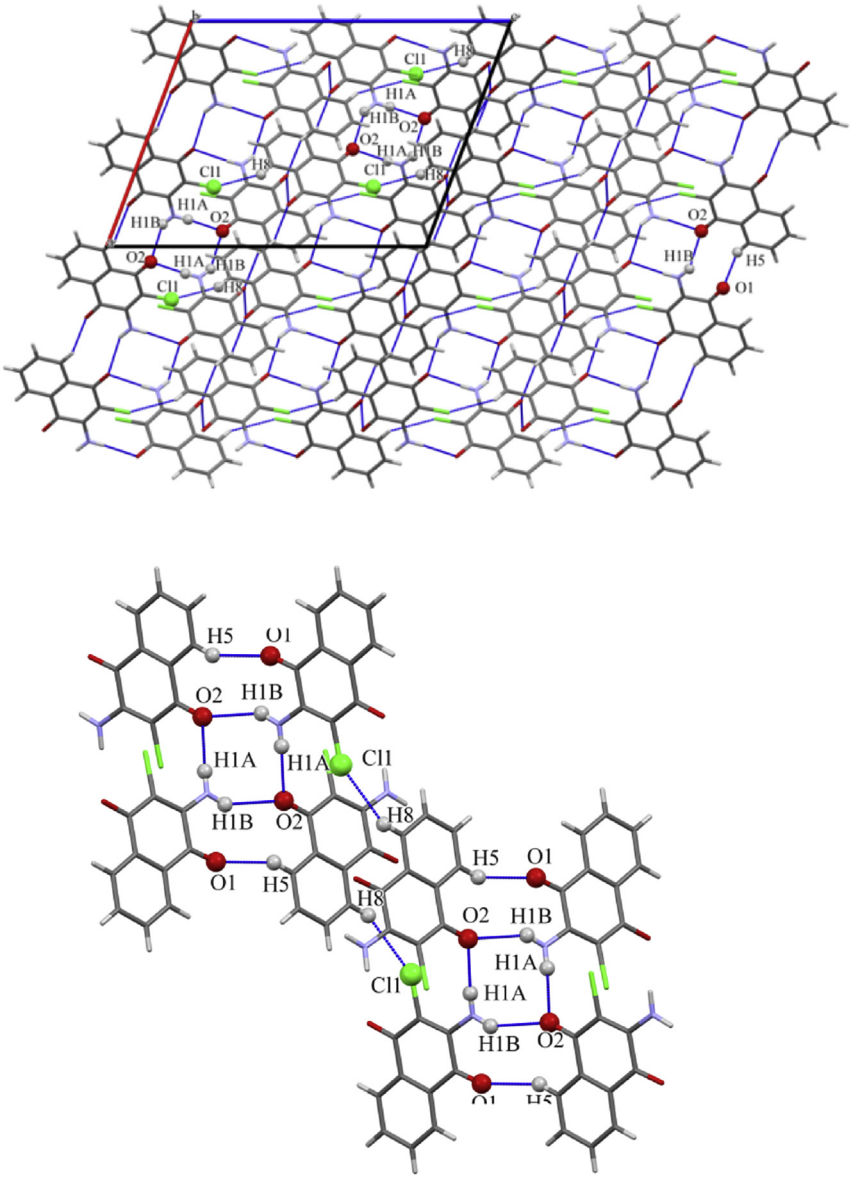

Fig. 7. Tetramer unit of compound 'B2' formed by N–H···O and C–H···O interaction down b-axis.

[27]. The structure given by Métras [26] showed that the crystal belongs to the triclinic *P-1*, space group (A1). The crystals were obtained from toluene, showed the cell parameters, a = 18.18 Å (α = 112° 30′), b = 8.29 Å (β = 73°) and c = 7.35 Å (γ = 117° 30′). There are two molecules in unit cell and the centroid of every alternate molecule revealed π-π stacking interactions (~3.50 Å) between the symmetry equivalent molecules when viewed down b-axis (Fig. 2a). The molecules possess Cl···O close contacts (Fig. 2b) as well. Orthorhombic polymorph (A2) with space group

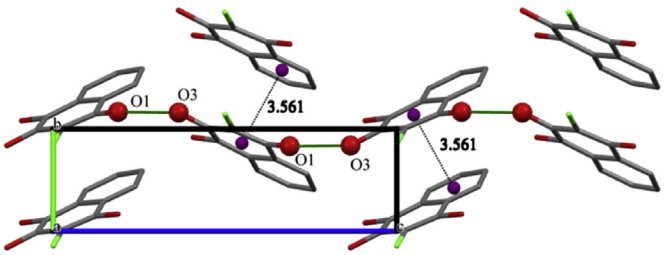

Fig. 8. Chlorolawsone polymorph 'C1' (*Pc*) molecules down c-axis.

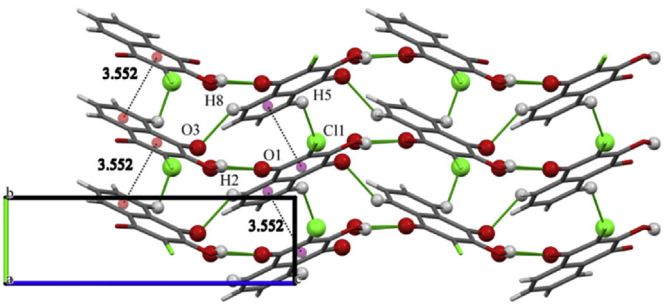

Fig. 9. π-π stacking of symmetry equivalence polymorph C2 chains down a-axis.

Pb2₁a obtained from the melt of dichlone by Ikemoto et al. [27] in 1977. The cell parameters turns out to be a = 16.204(12)Å, b = 26.686(17) Å (β = 113°) and c = 3.830(2) Å. Molecules are denoted by 'X1' and Y1′(Fig. S1 in ESI†). Chlorine, Cl(1) and Cl(2) of molecule 'X1' showed Cl···O close contacts, while molecule Y1 only Cl(3) facilitate Cl···O close contacts (Fig. 3). Dimeric chains of X1 and Y1, formed by C—H···O, C—H···Cl interaction and Cl···O close contacts engendering extended polymeric chain as be viewed down the c-axis.

Polymorph of dichlone in the present work (A3) was obtained from the unreacted fraction (of the column chromatography) of the reaction of 2-aminophenol and dichlone, with toluene and methanol as eluents. A parrot green color crystals belongs to triclinic space group *P-1*(A3) with cell parameters being a = 7.3279(1) Å, (α = 89.769(1)°), b = 8.2765(1) Å, (β = 82.542(1)°) and c = 16.1368(3) Å (γ = 67.0180(6)°). The cell parameters differed from those of Métras [26]. Two molecules in the asymmetric unit are denoted by 'X' and 'Y'.

Molecules 'X' and 'Y' differ with respect to intermolecular hydrogen bonding. Each molecule of 'X' is in close contact with four 'Y' and other two 'X' molecules. Further each molecule 'Y' in vicinity to four 'X' and two other 'Y' molecules. The X and Y molecules differed with respect to intermolecular C—H···O hydrogen bonding interactions from.

C(6)—H(6)···O(2′) in molecule X and C(7′)-H(7′)···O(1) in molecule Y. The interactions from the O(2) and O(1′), respectively of X and Y are absent.

The C—H···O and C—H···Cl interactions in both molecules (X and Y) form a planar sheet (Fig. 4) and π-π stacked interactions can be noticed on viewing down the b-axis in Fig. 5. The centroid separations of π-π stacked X···X molecules turned out to be 3.53 Å and 3.50 Å in Y···Y molecules. The interlayer spacing of symmetry equivalent molecules varies and the centroid distance was turned out to be 4.619 Å between 'X' molecules and 4.173 Å for 'Y' molecules (Fig. 5).

Molecular structure of polymorph of B1 was reported by Hauw et al. [31] in 1965 (polymorph B1). The crystals obtained in acetic acid revealed monoclinic space group, *Pc* and the cell parameters are a = 8.11(2)Å, b = 3.93(2)Å, (β = 113°) and c = 14.84(2)Å. When viewed down a-axis (Fig. 6) molecules showed N—H···O interaction (N(1)···O(1) = 2.849 Å). The polymeric chain further extends via π-π stacking (3.567 Å).

A polymorph of B2 obtained in the present work (polymorph B2) by reaction of dichlone and aqueous ammonia and purified by column chromatography with ether-ethyl acetate as eluent solvent (named as B2). As may be noticed 'B2' crystallizes in monoclinic *C2/c* space group (Fig. 1) with eight molecules in its unit cell. Each molecule is in vicinity to six neighbouring molecules via N—H···O,

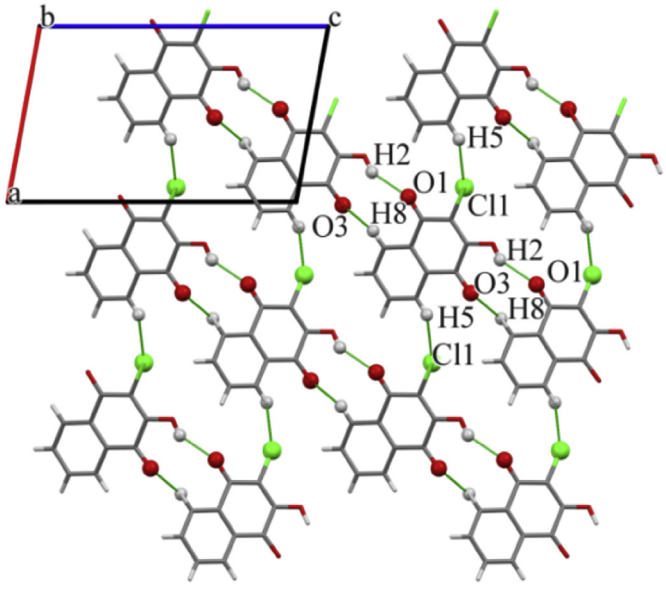

Fig. 10. Polymeric chain formed by O—H···O and C—H···O of 'C2' polymorph also showed inter chain C—H···Cl interaction down b-axis.

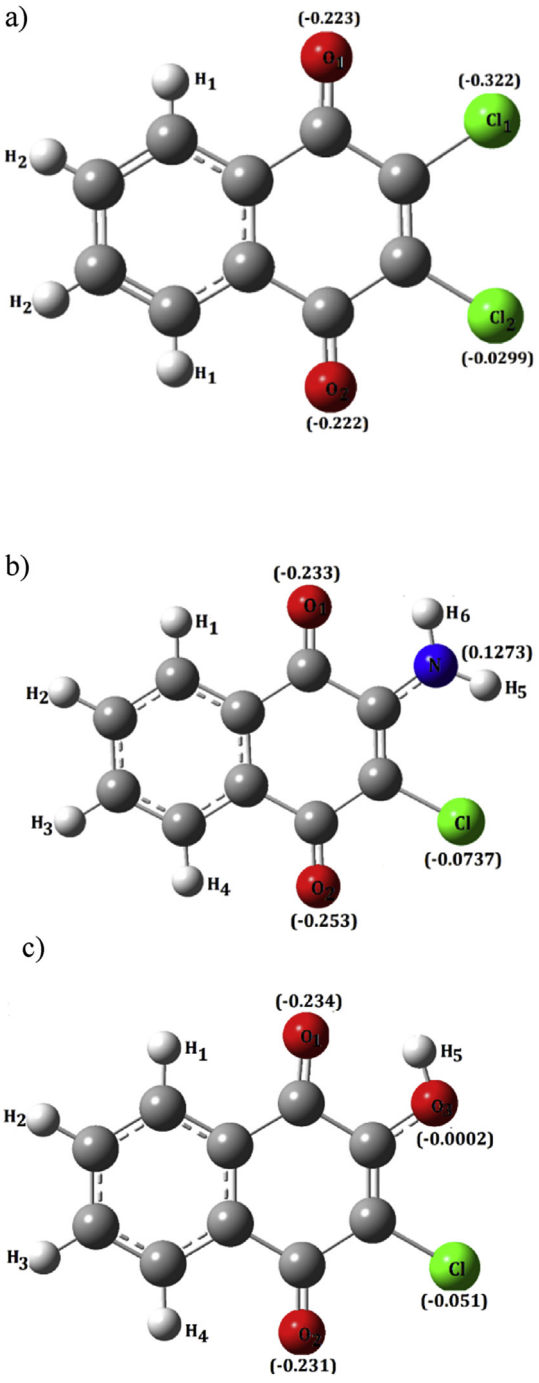

Fig. 11. Optimized structures of monomer (a) A3, (b) B2 (c) C2. Atomic labeling scheme is also shown along with.

C–H···O and C–H···Cl (Fig. S2 in ESI†) intermolecular interactions. Oxygen O(2) as well as the H(11A) and H(11B) showed bifurcated N–H···O interaction. Polymeric chain is facilitated by N(11)–H(1B)···O(2) and C(5)–H(5)···O(1) interactions. A tetrameric unit of molecules was resulted from N–H···O interactions with N–H(11A)···O(2)(1/2 + x, 1/2 + y,z) and N–H(11B)···O(2) (1/2−x,−1/2 + y, 1/2−z) from the two parallel chains running in opposite directions when viewed down the b-axis. The tetrameric units are further joined by CH···Cl interactions (Fig. 7) viz., N(11)-H(1A)···O(2) (1/2−x, ½+y, ½−z) and C(8)–H(8)···Cl(1) (x,2−y, 1/2 + z).

Crystal structure of chlorolawsone has been known since 1965 by Hauw et al. [29] (polymorph C1). The crystals obtained by sublimation of the solid showed monoclinic space group *Pc* with one molecule in asymmetric unit. The cell parameters are a = 8.25(2) Å, b = 3.92(2) Å (β = 113.20°) and c = 14.39(3) Å. The molecules showed polymeric chain formed via O–H···O interaction, when viewed down c-axis (Fig. 8) with O(1)···O(3) separations being 2.750 Å. The neighbouring polymeric chains reveal π-π stacking interactions between quinonoid and benzenoid ring with centroid being separated by 3.561 Å.

The crystals of C2 were obtained in methanol in our laboratory belong to monoclinic crystal system and the space group is *Pn* (Fig. 1). The cell parameters are a = 8.25530(15), b = 3.90730(15), c = 13.4222(2) and β = 100.4200(8)° and there is one molecule in the asymmetric unit. Each molecule is in vicinity to eight neighbouring molecules facilitating O–H···O, C–H···O and C–H···Cl interactions besides π-π stacking. Thus polymeric chain extends through O(2)–H(2)···O(3) and C(8)–H(8)···O(3) interactions (Fig. 9) when viewed down a-axis. The polymeric chains are connected by C(5)–H(5)···Cl(1)) interactions (Fig. 10) can be seen down b-axis. The neighbouring chains are stabilized owing to π-π stacking interactions (Fig. 9) between benzenoid and quinonoid rings.

3.3. DFT investigations

Optimized structures of monomer 'A3', 'B2' and 'C2' from the density functional theory are portrayed in Fig. 11. The net atomic charges derived from the population analyses based on Hirshfeld partitioning scheme are given in parentheses. Structural parameters of local minima on the potential energy surface agree fairly well with those observed in the X-ray crystal data (*cf* Table 4). To understand interplay between halogen and hydrogen bonding we delve into dimer formation by 'A3', 'B2' and 'C2' conformers. Optimized dimers are shown in Fig. 12.

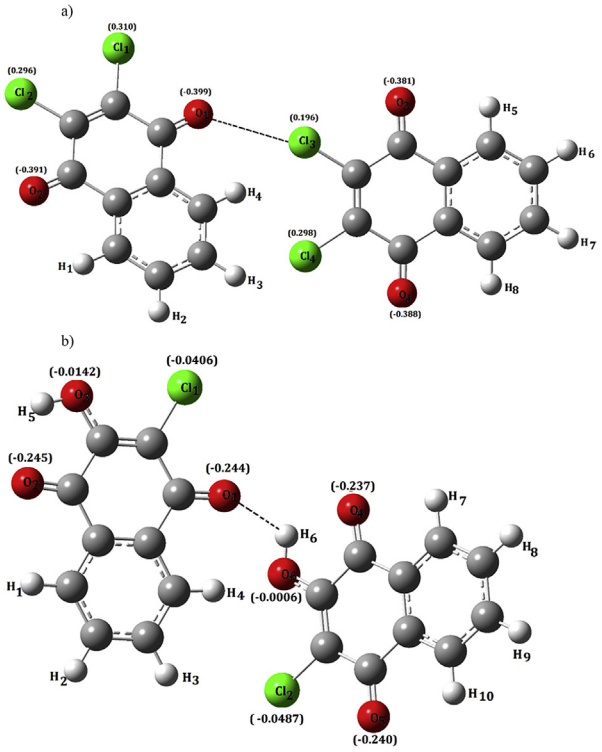

Fig. 12. Optimized structures of dimer (a) A3, (b) C2. Atomic labeling scheme is also shown along with.

The present theoretical calculations revealed that 'A3' and 'C2' tend to form dimer species; the corresponding binding energies turned out to be 7.0 kJ mol^{-1} and 17.5 kJ mol^{-1}, respectively. As opposed to this the conformer 'B2' does not favor dimer formation and calculated binding energies turn out to be largely negative (−63 kJ mol^{-1}). These inferences are in consonance with the X-ray crystal structure experiments. Noteworthy enough, the dimer 'A3' possess Cl···O close contacts (the separation being 3.1 Å). The dimer C2 on the other hand, are rendered with the O–H···O (2.20 Å) hydrogen bonding. The density functional theoretic structures thus corroborate inferences drawn from the single crystal X-ray diffraction experiments. To simulate the influence of

Table 4
Selected bond distances (in Å) in A3 and C2 dimer in the gas phase and in methanol.

	A3		C2	
	Gas	Methanol	Gas	Methanol
C–Cl(1)	1.718	1.709	1.76	1.76
C–Cl(2)	1.712	1.713	1.76	1.76
C–Cl(3)	1.708	1.703		
C–Cl(4)	1.727	1.706		
C=O(1)	1.210	1.204	1.258	1.258
C=O(2)	1.215	1.205	1.258	1.257
C=O(3)	1.218	1.204	1.258	1.258
C=O(4)	1.222	1.209	1.258	1.258
C–H(1)	1.087	0.929	1.070	1.070
C–H(2)	1.082	0.931	1.070	1.070
C–H(3)	1.087	0.930	1.070	1.070
C–H(4)	1.082	0.929	1.070	1.070
C–H(5)	1.083	0.929	1.070	1.070
C–H(6)	1.089	0.930	1.070	1.070
C–H(7)	1.085	0.930	1.070	1.070
C–H(8)	1.081	0.930	1.070	1.070
O–H(5)			0.96	0.96
O–H(6)			0.96	0.96

Table 5
The comparison of experimental and calculated vibrational frequencies (scaled by 0.9657) in cm^{-1} of A3, B2 and C2. The experimental values are given in parenthesis.

	A3(dimer)	B2 (monomer)	C2(dimer)
ν(CH)	3165, 3127	3121(3294)	3199(3268)
		3111(3109, 2977)	3110
ν(C=O_1)	1776(1776)	1646(1678)	1733
ν(C=O_2)	1747(1703)	1819	1760(1865)
ν(C=O_3)	1730(1678)		1704(1765)
ν(C=O_4)	1704		1698(1699, 1669, 1640)
ν(C=C)	1634	1656(1591, 1552)	1636(1584)
ν(NH_2)		3618(3474)	
		3612	
ν(O_3H)			3627(3736)
ν(O_6H)			3538(3674)

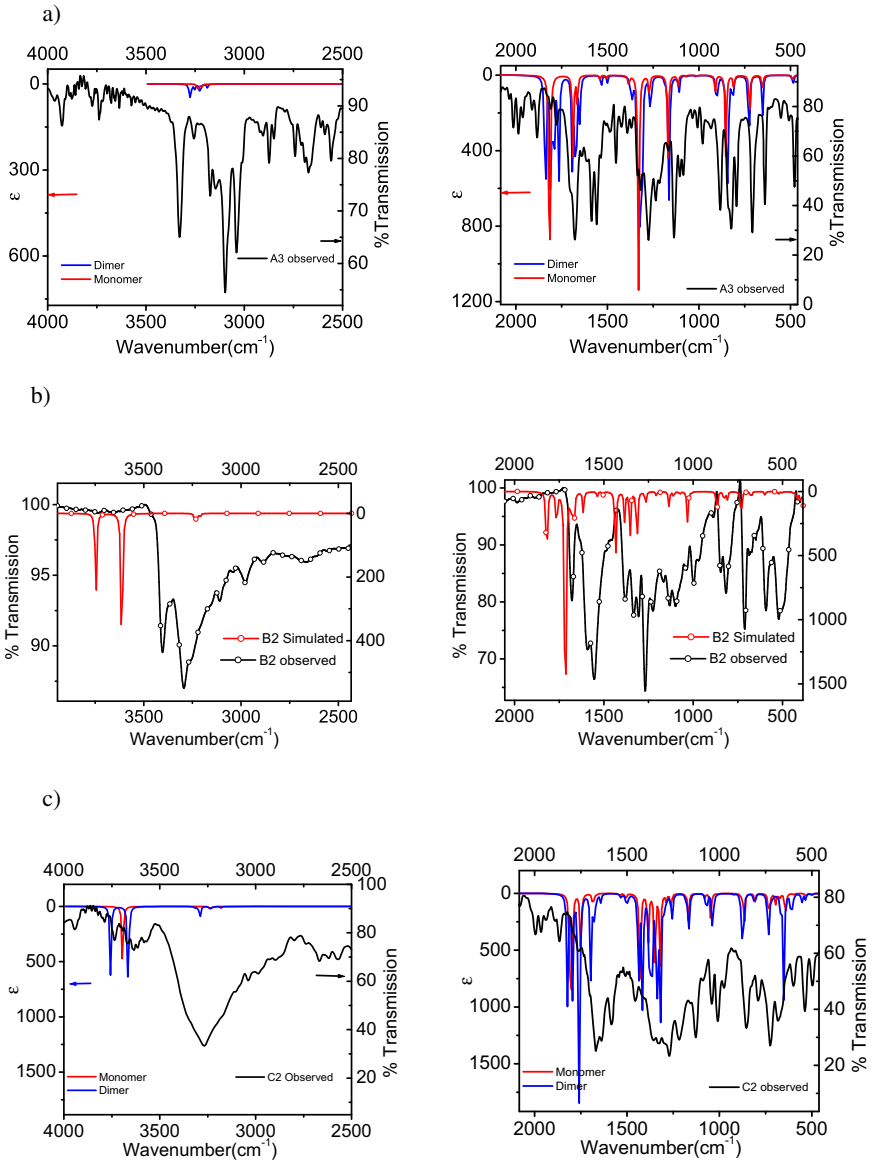

Fig. 13. Optimized and observed IR spectra of a) 'A3', b) 'B2' and c) 'C2'.

solvent on the structure of these dimers we further carried out the SCRF-PCM calculations using methanol as the solvent. The structural parameters obtained are displayed in Table 4. Structural ramifications of such interactions in vibration frequencies can further be probed through the normal vibration analysis. A comparison of calculated vibrational frequencies (scaled by a factor of 0.9657) of the monomer 'B2' and dimers 'A3' and 'C2' with those observed has been given in Table 5. Theoretical computed spectra are also compared with those measured in experiment in Fig. 13.

^{1}H NMR chemical shifts in monomers as well as those in dimers in DMSO were simulated through the SCRF-PCM theory at the M06-2x/6-31++G(d,p) level of theory. Overall the calculated δ_H values (Table 6) are in consonance with experiments and generally exhibit larger deshielding relative to those measured in the experiment. Frontier orbitals HOMO and LUMO of A3, B2, C2 dimers portrayed in Figs. 14 and 15 revealed the electron-rich regions localized exclusively on one of the monomer. The complementarily of electronic distributions can be noticed in these orbital's. Moreover, the Time Dependent Density Functional Theory (TDDFT) calculations revealed several bands in the electronic spectra of 'A3', 'B2' and 'C2' in the gas phase and in methanol agree well with experiment. The MO's and assignments of electronic transitions in the UV spectra of

Table 6
^{1}H chemical shift (in ppm) in DMSO for monomer and dimer values. The experimental values are given in parenthesis.

	A3 monomer	B2 monomer	C2 monomer	A3 dimer	C2 dimer
H(1)	9.4(8.18)	9.2(8.16)	9.2	9.1	9.2(8.00)
H(2)	8.9(7.8)	9.2(7.65)	9.2	9.5	8.9(7.86-7.74)
H(3)		9.5(7.70)	9.5	9.3	9.2(8.00)
H(4)		9.4(8.17)	9.6	10.3	10.7(7.86-7.74)
H(5)		6.2(5.5)	8.2	9.5	8.5(3.89)
H(6)		6.8(5.5)		9.1	10.7
H(7)				8.9	9.4
H(8)				9.5	9.5
H(9)					9.6

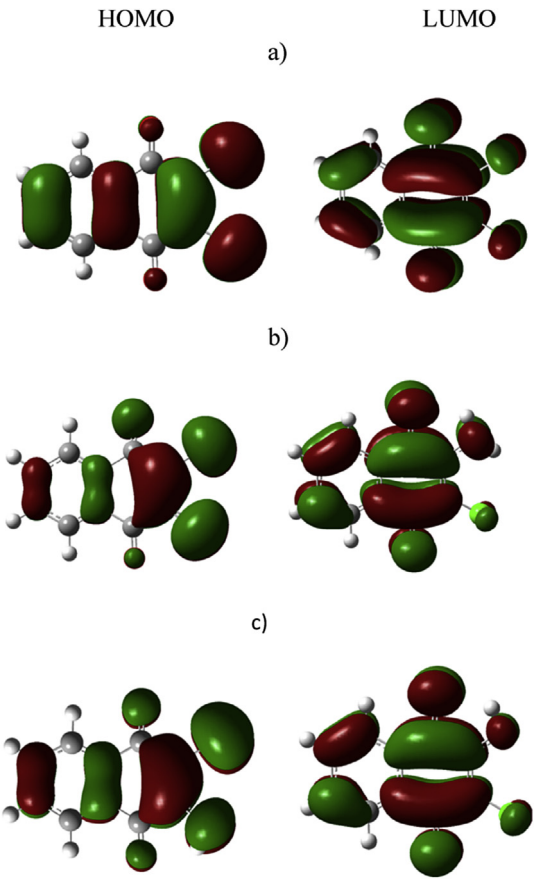

Fig. 14. Frontier orbital's (HOMO and LUMO) in monomer (a) A3 (b) B2 and (c) C2.

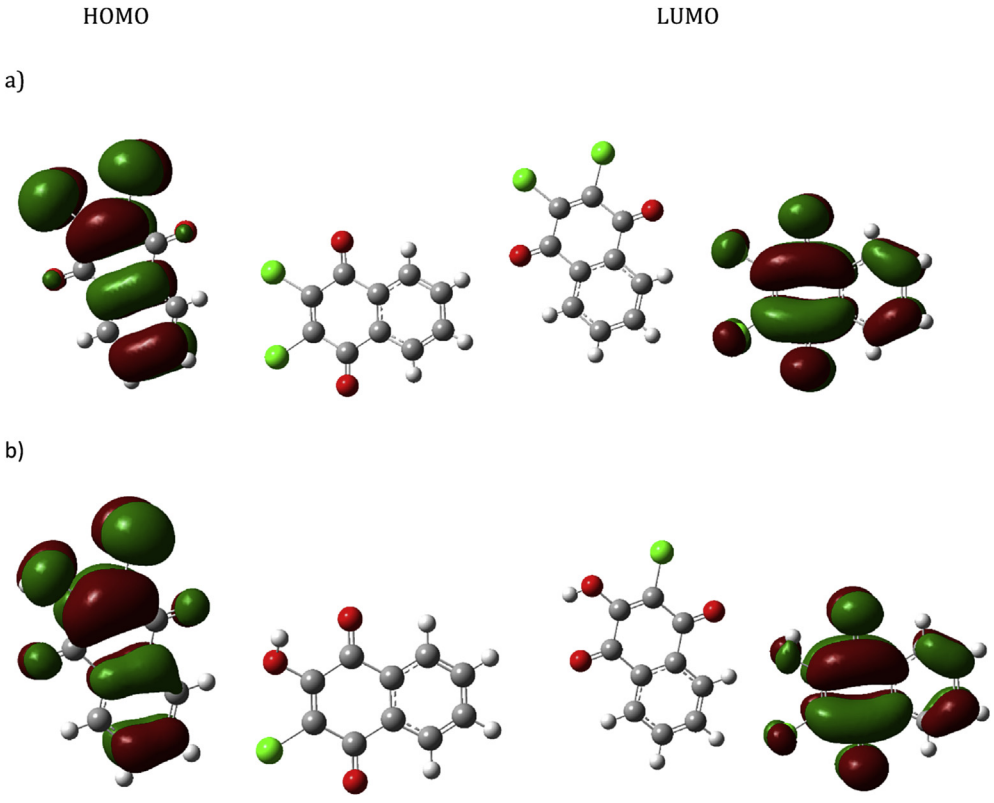

Fig. 15. Frontier orbital's (HOMO and LUMO) in dimer (a) A3 and (b) C2.

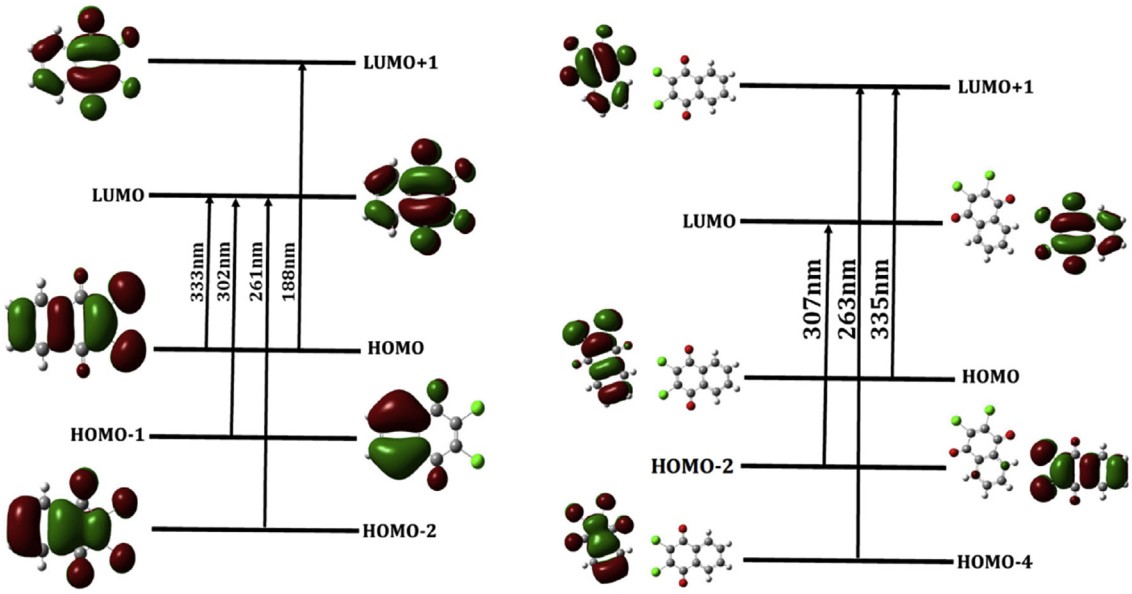

Fig. 16. MO diagram explaining the electronic spectra of A3 monomer (left) and A3 dimer (right).

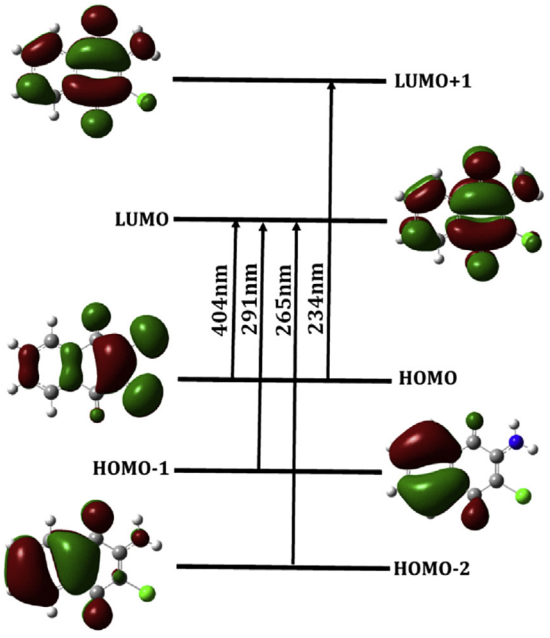

Fig. 17. MO diagram explaining the electronic spectra of B2 monomer.

A2, B2 and C2 from the TDDFT theory has been shown in Figs. 16–18. The wavelength maxima (λ_{max}), oscillator strength (*f*) along with excitation energies (E_{ex}) of A3 and C2 are summarized in Tables 7a and b. The absorption band near 307 nm of the dimer A arises from the (HOMO-2) to LUMO transition.

4. Conclusions

Compound A: 2,3-dichloro-1,4-naphthoquinone possess three polymorphs viz. triclinic *P-1* (A1 and A3), orthorhombic; $Pb2_1a$ (A2). Compound B: 2-amino-3-chloro-1,4-naphthoquinone showed two polymorphs monoclinic *Pc* (B1) and $C_{2/C}$ (B2). Compound C: 2-chloro-3-hydroxy-1,4-naphthoquinone crystallizes as two polymorphs in triclinic *Pc* (C1) and *Pn* (C2). Structural parameters, spectral characteristics observed in infrared, ^{1}H NMR, UV–visible spectra are presented. The dispersion corrected M06-2x density functional calculations showed that the compound A3 possesses halogen bonding interactions while the crystalline network in C2 extends through hydrogen bonding interactions. Compound B2 void of both such interactions does not favor dimer formation. TDDFT has been used to assign the transitions in the electronic spectra.

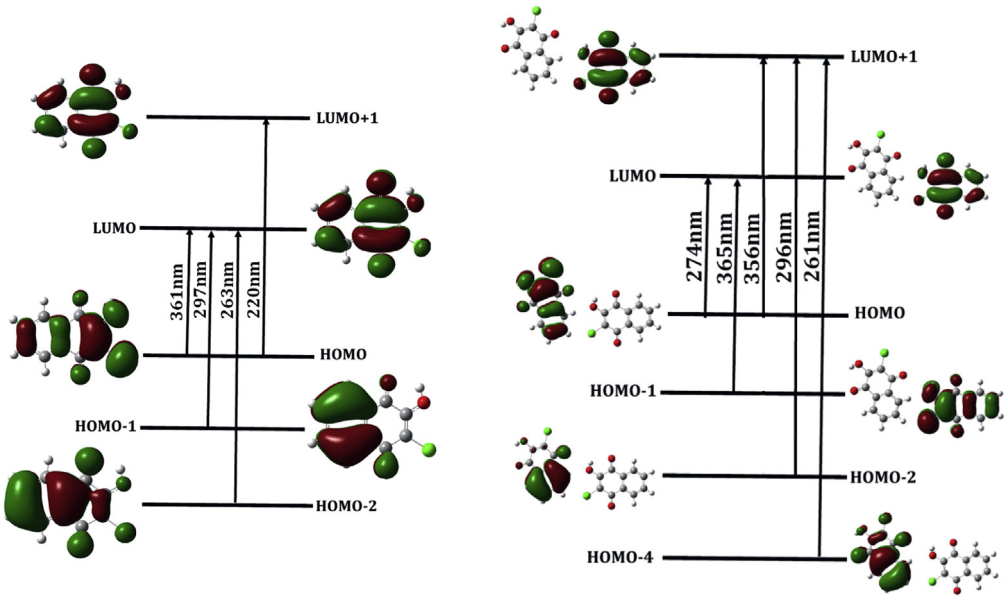

Fig. 18. MO diagram explaining the electronic spectra of C2 monomer (left) and C2 dimer (right).

Table 7a
Wavelength maxima (λ_{max}, nm), oscillator strengths (f) and assignments of bands in the electronic spectra of the monomer A3, B2, and C2 in methanol from TDDFT. The experimental values are given in parenthesis.

Transition	A3			B2			C2		
	E_{ex}(eV)	λ_{max} (nm)	(*f*)	E_{ex}(eV)	λ_{max} (nm)	(*f*)	E_{ex}(eV)	λ_{max} (nm)	(*f*)
Homo→Lumo	3.7	333(339)	0.0069	3.1	404(449)	0.0611	3.5	361(321, 472)	0.0293
Homo-1→ Lumo	4.2	302(289)	0.1047	4.3	291(332)	0.0943	4.2	297(287)	0.1121
Homo-2 →Lumo	4.8	261	0.3885	4.7	265(284)	0.2971	4.7	263	0.3565
Homo→ Lumo+1	6.6	188	0.3050	5.3	234	0.4588	5.6	220	0.4596

Table 7b
Wavelength maxima (λ_{max}), oscillator strengths (*f*) and assignments of bands in the electronic spectra of the dimer A3, and C2 in methanol from TDDFT. The experimental values are given in parenthesis.

Transition	A3			C2		
	E_{ex}(eV)	λ_{max}(nm)	(*f*)	E_{ex}(eV)	λ_{max}(nm)	(*f*)
Homo → Lumo				4.5	274(287)[a]	0.0877
Homo-4 → Lumo+1	5.0	263	0.5003	4.7	261	0.2516
Homo-2 → Lumo	4.0	307 (289)	0.1292			
Homo → Lumo+1	3.7	335(339)	0.0082	3.5	356(321)	0.0213
Homo-1 → Lumo				3.4	365	0.0284
Homo-2 → Lumo+1				4.2	296	0.1214

[a] Experimental values.

Acknowledgements

SSG is grateful to ISRO Project 136 ("Naphthoquinone containing metal polypyridyl complexes for Solar Cells: Computational and experimental Study") India for financial support. DC acknowledge University Grants Commision (UGC), New Delhi, India for Meritorious fellowship. SPG acknowledges the support from the Board of Research in Nuclear Sciences, India in the form of the research project (37(2)/14/11/2015-BRNS). DNL is thankful to Savitribai Phule Pune University for the award of research fellowship through the University of potential excellence scheme from the UGC, New Delhi, India.

Appendix A. Supplementary data

Supplementary data related to this article can be found at http://dx.doi.org/10.1016/j.molstruc.2016.05.022.

References

[1] H.G. Brittain, Polymorphism in Pharmaceutical Solids, Marcel Dekker, New York, 1999.
[2] M.C. Etter, S.M. Reutzel, J. Am. Chem. Soc. 113 (1991) 2586–2598.
[3] G.R. Desiraju, J.J. Vittal, A. Ramanan, Crystal Engineering, World Scientific Publishing Co. Pte. Ltd, 2011, p. 34.
[4] B. Rodríguez-Sponga, C.P. Price, A. Jayasankar, A.J. Matzgerb, N. Rodríguez-Hornedo, Adv. Drug Deliv. Rev. 56 (2004) 241–274.

[5] X. Yang, B. Fu, B. Yu, J. Am. Chem. Soc. 133 (2011) 12433–12435.
[6] K.W. Wellington, RSC Adv. 5 (2015) 20309–20316.
[7] M. Saibu, S. Sagar, I. Green, F. Ameer, M. Meyer, Org. Biomol. Chem. 6 (2008) 637–656.
[8] P. Dowd, R. Hershline, S.W. Ham, S. Naganathan, Nat. Prod. Rep. 11 (1994) 251–264.
[9] A. Voskiene, B. Sapijanskaite, V. Mickevicius, K. Kantminiene, M. Stasevych, O. Komarovska-Porokhnyavets, R. Musyanovych, V. Novikov, Monatsh. Chem. 142 (2011) 529–537.
[10] M. Ángeles Castro, A.M. Gamito, V. Tangarife-Castano, B. Zapata, J.M. Miguel del Corral, A.C. Mesa-Arango, L. Betancur-Galvis, A.S. Feliciano, Eur. J. Med. Chem. 67 (2013) 19–27.
[11] S. Pal, V.B. Konkimalla, L. Kathawate, S.S. Rao, S.P. Gejji, V.G. Puranik, T. Weyhermüller, S. Salunke-Gawali, RSC Adv. 5 (2015) 82549–82563.
[12] D. Chadar, S.S. Rao, A. Khan, S.P. Gejji, K.S. Bhat, T. Weyhermüller, S. Salunke-Gawali, RSC Adv. 5 (2015) 57917–57929.
[13] L. Kathawate, P.V. Joshi, T.K. Dash, S. Pal, M. Nikalje, T. Weyhermüller, V.G. Puranik, V.B. Konkimalla, S. Salunke-Gawali, J. Mol. Struc. 1075 (2014) 397–405.
[14] D. Chadar, M. Camilles, R. Patil, A. Khan, T. Weyhermüller, S. Salunke-Gawali, J. Mol. Struc. 1086 (2015) 179–189.
[15] R. Patil, D. Chadar, D. Chaudhari, J. Peter, M. Nikalje, T. Weyhermüller, S. Salunke-Gawali, J. Mol. Struc. 1075 (2014), 375–351.
[16] O. Pawar, A. Patekar, A. Khan, L. Kathawate, S. Haram, G. Markad, V. Puranik, S. Salunke-Gawali, J. Mol. Struc. 1059 (2014) 68–74.
[17] N.E. Newell, R.J. Mazaika, W.J. Cook, J. Agric. Food. Chem. 6 (1958) 669–671.
[18] W.P.T. Horst, E.L. Felix, Ind. Eng. Chem. 35 (1943) 1255–1259.
[19] C. Graebe, Ber 1 (1867) 36.
[20] E. Carstanjen, Ber 2 (1868) 633.
[21] A. Ceccaldi, A. Rajavelu, S. Ragozin, C. Sénamaud-Beaufort, P. Bashtrykov, N. Testa, H. Dali-Ali, C. Maulay-Bailly, S. Amand, D. Guianvarch, A. Jeltsch, P.B. Arimondo, ACS Chem. Biol. 8 (2013) 543–548.
[22] S.-C. Kuo, T.I. buka, L.-J. Huang, J.-C. Lien, S.-R. Yean, S.-C. Huang, D. Lednicer, S. Morris-Natschke, K.-H. Lee, J. Med. Chem. 39 (1996) 1447–1451.
[23] J.A. VanAllan, A.R. Reynolds, J. Org. Chem. 28 (1963) 1019–1022.
[24] C. Ibis, A.F. Tuyun, H. Bahar, S.S. Ayla, M.V. Stasevych, R.Y. Musyanovych, O. Komarovska-Porokhnyavets, V. Novikov, Med. Chem. Res. 23 (2014) 214d0–2149.
[25] M.F. Sartori, Chem. Rev. 63 (1963) 279–296.
[26] J.-C. Métras, Acta Cryst. 14 (1961) 153.
[27] I. Ikemoto, K. Yakushi, Y. Naito, H. Kuroda, Acta Cryst. B33 (1977) 2076–2079.
[28] J.B. Conant, L.F. Fieser, J. Am. Chem. Soc. 46 (1924) 1858–1881.
[29] J. Gaultier, C. Hauw, Acta Cryst. 19 (1965) 580–584.
[30] K. Fries, P. Ochwat, ibid 66 (1923) 1291.
[31] J. Gaultier, C. Hauw, Acta Cryst. 19 (1965) 585–590.
[32] D.D. Perrin, W.L. Armarego, D.R. Perrin, Purification of Laboratory Chemicals, Pergamon Press, London, 1988, p. 260.
[33] J.R.E. Hoover, A. Day, J. Am. Chem. Soc. 76 (1954) 4148–4152.
[34] Bruker, APEX2, SAINT, and SADABS, Bruker AXS Inc., Madison, Wisconsin, USA, 2007.
[35] G.M. Sheldrick, Acta Cryst. A64 (2008) 112–122.
[36] L.J. Farrugia, J. Appl. Cryst. 45 (2012) 849–854.
[37] C.F. Macrae, I.J. Bruno, J.A. Chisholm, P.R. Edgington, P. McCabe, E. Pidcock, L. Rodriguez Monge, R. Taylor, J. van de Streek, P.A. Wood, J. Appl. Crystallogr. 41((2008) 466–470.
[38] A.L. Spek, Acta Cryst. D65 (2009) 148–155.
[39] M.J. Frisch, G.W. Trucks, H.B. Schlegel, G.E. Scuseria, M.A. Robb, J.R. Cheeseman, J.A. Montgomery Jr., T. Vreven, K.N. Kudin, J.C. Burant, J.M. Millam, S.S. Iyengar, J. Tomasi, V. Barone, B. Mennucci, M. Cossi, G. Scalmani, N. Rega, G.A. Petersson, H. Nakatsuji, M. Hada, M. Ehara, K. Toyota, R. Fukuda, J. Hasegawa, M. Ishida, T. Akajima, Y. Honda, O. Kitao, H. Nakai, M. Klene, X. Li, J.E. Knox, H.P. Hratchian, J.B. Cross, V. Bakken, C. Adamo, J. Jaramillo, R. Gomperts, R.E. Stratmann, O. Yazyev, A.J. Austin, R. Cammi, C. Pomelli, J.W. Ochterski, P.Y. Ayala, K. Morokuma, G.A. Voth, P. Salvador, J.J. Dannenberg, V.G. Zakrzewski, S. Dapprich, A.D. Daniels, M.C. Strain, O. Farkas, D.K. Malick, A.D. Rabuck, K. Raghavachari, J.B. Foresman, J.V. Ortiz, Q. Cui, A.G. Baboul, S. Clifford, J. Cioslowski, B.B. Stefanov, G. Liu, A. Liashenko, P. Piskorz, I. Komaromi, R.L. Martin, D.J. Fox, T. Keith, M.A. Al-Laham, C.Y. Peng, A. Nanayakkara, M. Challacombe, P.M.W. Gill, B. Johnson, W. Chen, M.W. Wong, C. Gonzalez, J.A. Pople, Gaussian03, Revision, Gaussian, Inc., Pittsburgh, PA, 2003.
[40] Y. Zhao, D.G. Truhlar, Acc. Chem. Res. 41 (2008) 157–167.
[41] Y. Zhao, N.E. Schultz, D.G. Truhlar, J. Chem. Theory Comput. 2 (2006) 364.
[42] Y. Zhao, D.G. Truhlar, J. Chem. Theory Comput. 1 (2005) 415–432.